Journal of MATERIALS RESEARCH

Article
DOI:10.1557/s43578-023-01273-6

Processing of diamond films with azimuthal texture on silicon wafer for quantum systems

Vidhya Sagar Jayaseelan[1,2], Raj N. Singh[2,a)]

[1] Present Address: Intel Corporation, 8695 NE Cornell Rd, Hillsboro, OR 97124, USA
[2] School of Materials Science and Engineering, Oklahoma State University, 700 N. Greenwood Avenue, HRC-200, Tulsa, OK 74106, USA
[a)] Address all correspondence to this author. e-mail: Rajns@okstate.edu

Received: 8 May 2023; accepted: 11 December 2023

Diamond is a wide bandgap semiconductor possessing unique properties for applications in quantum systems and ultra-wide bandgap electronics, which require a fundamental understanding of processing of high-quality diamond crystals and textured films by microwave plasma-enhanced chemical vapor deposition (MPECVD). The approach of bias-enhanced nucleation (BEN) followed by growth is studied for processing of oriented diamond film with azimuthal texture. The magnitude of the applied electric field is shown to play an important role in processing of the highly azimuthally textured diamond film on Si (100) substrate. The X-ray diffraction pole figure, scanning electron microscopy, and Raman spectroscopy results show that an optimum applied electric field during BEN and microwave plasma conditions lead to formation of diamond film with azimuthal texture upon growth by MPECVD. These results are promising for fabricating diamond films of optimum characteristics containing nitrogen vacancy (NV) defect centers for application in quantum devices.

Introduction

Diamond has exceptional properties such as wide bandgap, high dielectric breakdown strength, optical transparency, and high thermal conductivity thereby making it an ideal material for quantum and optical devices as well as thermal management of electronics [1–6]. The diamond containing nitrogen vacancy (NV) defect centers shows novel properties for applications in quantum computing, quantum entanglement, encryption, bio-labeling, and magnetic field sensing [7–11]. Nitrogen vacancy (NV) centers in diamond have also attracted significant attention as well for bio-sensing, quantum information processing, and NMR (Nuclear Magnetic Resonance) spectroscopy [12–14]. Qubit states from spins of NV centers can be controlled by microwave and optical signals, thereby rendering quantum network, quantum memory, and quantum sensing [11, 15–18].

Most of the research on NV centers in diamond have used commercial HPHT (high-pressure high-temperature) single crystal diamond, and NV centers have been created by ion implantation followed by annealing at very high temperatures (1500 °C) to activate NV defects. This approach also creates more defects due to ion implantation. In another approach, diamond film is grown on tiny HPHT diamond crystals using MPECVD where nitrogen can be doped in situ for creating NV defects. There is also a need to explore processing of textured polycrystalline diamond films and doping it with nitrogen in situ for creating NV defects. This approach is more attractive because diamond films can be processed over wide areas on different substrates for many quantum applications. This approach is being explored in our research and this paper is a part of the overall program.

The NV centers in diamond are generally oriented randomly along four possible < 111 > directions. However, there is a need and challenge for preferentially aligning NV centers along one of the four < 111 > directions. The oriented or aligned NV centers are desirable for enhancing detectability for quantum application using Optically Detected Magnetic Resonance (ODMR). We are addressing this challenge through our fundamental research on texturing of the diamond films in situ through the bias-enhanced nucleation (BEN) and then by growth using MPECVD. This approach also requires a fundamental understanding of the role of the diamond nucleation and growth mechanisms on Si substrates to achieve the goal of textured diamond film. We first describe how diamond is generally processed in MPECVD, which is then followed by description of

the important role of BEN, in situ doping, and growth leading to textured diamond film containing aligned NV defects.

Diamond powder is used generally as abrasive for grinding and polishing applications, which is processed at HPHT where it is thermodynamically stable. Diamond is also processed at low pressures in an activated plasma environment typical of a MPECVD. Diamond containing NV defects can be processed using different approaches such as detonation synthesis for diamond particles and HPHT for small diamond crystals [19–21]. MPECVD is the most promising approach for synthesizing diamond film over a wider area on different substrates including on HPHT-synthesized single crystal diamond. MPECVD offers superior control of diamond phase purity and crystalline defects as described in our research [2, 22–30] and of many other researchers [31–43].

Diamond containing NV centers can be fabricated by in situ doping with nitrogen (N) or ammonia (NH_3) during MPECVD. This approach requires a fundamental understanding of the diamond nucleation and growth steps. It is known that diamond does not nucleate homogeneously on most solid substrates because of the barrier to nucleation from high surface energy. Therefore, heterogeneous nucleation is encouraged for processing continuous diamond films on Si or other substrates by MPECVD. It can be done by one of three ways, i.e., (1) scratching the surface, (2) ultrasonic agitation with diamond particles, and (3) seeding of the surface with nanodiamond particles. These approaches are used to facilitate heterogeneous nucleation sites followed by growth on already nucleated diamond. Narayan's group nucleated and grew diamond from carbon films by a novel approach of laser irradiation [4–6]. In this approach, a new phase of caron, Q-carbon, is created within the amorphous carbon, which promotes formation of diamond of different morphologies on Si and sapphire substrates [6]. They suggested that diamond can nucleate on these substrates upon laser irradiation because the large concentration of sp^3 clusters within the Q-carbon because of supercooling and Gibb's free energy considerations. In addition, electrical bias-enhanced nucleation (BEN) in a plasma has been used for promoting nucleation in situ followed by growth to synthesize diamond thin films by MPECVD [31–35]. MPECVD approach in combination with the BEN also offers an independent control of the nitrogen doping via gaseous precursors of N_2 or NH_3 to grow diamond crystals and films for creating NV defect centers in situ of desired quality.

BEN approach has been used for enhancing nucleation and promoting heteroepitaxial growth of diamond on Si and other substrates by us and other researchers [31–35]. BEN followed by growth using MPECVD is the most promising approach for processing wafer scale diamond single crystal on Si substrates using Ir interlayer as clearly demonstrated by several researchers [44–46]. In the BEN approach, a thin layer of carbon is first deposited on the Si substrate followed by application of an electrical bias (100–300 V) in situ for a short duration (5–15 min), followed by growth, all in a MPECVD environment. Several mechanisms such as super saturation of carbon at the surface [35], enhanced surface mobility [36], faster reaction rate at the surface [37], formation of epitaxial layer of SiC on Si [38], and formation of a carbon layer that condenses to form epitaxial nuclei [39] have been suggested for the nucleation process. However, there is clearly no consensus among researchers on the mechanism of BEN although supporting evidences have been presented for each of these mechanisms, but they seem to contradict each other.

In a recent study, we have demonstrated that nucleation of diamond in the BEN approach occurs within the amorphous carbon film close to the Si (100) substrate and there is no evidence of SiC formation facilitating diamond nucleation by BEN [47]. This amorphous carbon film forms during carbonization step and before the BEN step in a MPCVD environment. Detailed characterization of the nucleating layer on Si (100) by HRTEM, selected area electron diffraction (SAED), and Raman spectroscopy provided supporting evidence of these claims [47]. The Raman spectroscopy from the amorphous carbon film that formed on Si (100) under MPECVD environment had broad Raman peaks near 1335 and 1505 cm^{-1} arising from the first-order phonon peak of diamond (sp^3 clusters) broadened by phonon confinement and I-band of amorphous carbon or sp^2 carbon clusters observed in nanocrystalline diamond, respectively, indicating that a significant amount of the sp^3-bonded carbon cluster formation even before the BEN step. Based on these and HRTEM supporting data, it was suggested that the epitaxial and oriented diamond nucleated on the Si (100) surface due to energetic plasma ion bombardment from biasing electric field and grew into textured diamond film upon further growth in the MPECVD environment. These findings are the basis of the research work described in this paper.

Therefore, the objective of this fundamental research is to study processing of diamond film on Si (100) substrate using BEN followed by growth in a MPECVD system leading to the formation of polycrystalline diamond film having grains with aligned azimuthal texture. This paper describes the role of the electric potential applied in situ during BEN and other MPECVD processing conditions on promoting azimuthally textured diamond film growth. The nature of the diamond film grown is characterized by XRD pole figure measurement, SEM, and Raman spectroscopy. The XRD pole figures and SEM results show that diamond film with excellent azimuthal texture can be processed on the Si (100) substrate under the influence of microwave and optimum level of the applied electric field during BEN that leads to textured diamond film and oriented crystals within upon further growth. The diamond film with excellent azimuthal texture is expected to be a promising host for promoting growth of the oriented NV centers in situ by MPECVD for a myriad of

applications in quantum systems and wide area growth of single crystal diamond [45–47].

Results and discussion

As indicated earlier, the role of processing conditions on the growth of textured diamond films was studied. Specifically, the influences of nucleation methods of BEN and ultrasonic agitation were investigated. In addition, the influence of applied voltage during BEN was also studied for processing textured diamond films. More details on the experimental methods are provided in a separate section after conclusions. These results are presented and discussed next in separate sections including perspective of this research on quantum applications and wide area growth of single crystal diamond.

Influence of nucleation methods on the texture of diamond films

Diamond films were deposited on Si (100) substrate following steps and conditions as described in the experimental section and Table 1. Two types of nucleation approaches were used. In the first case, BEN was used, and in the second case, ultrasonic agitation was applied. The SEM images from films grown after nucleation by the BEN and ultrasonic agitation techniques are shown in Fig. 1(a), (b). The sample nucleated by BEN for 5 min at 150 V bias shows [Fig. 1(a)] formation of the oriented pyramidal shape diamond grains on the silicon substrate with the diamond [110] edges parallel to the Si [110] and the diamond (100) planes parallel to the Si (100) planes. Each of the grains has a pyramidal shape with the square base of (100) planes parallel to the Si (100) planes and four pyramidal planes (111) forming the diamond crystals. This growth morphology of diamond crystals is consistent with the surface energies (γ) of different planes of diamond, i.e., γ (111) < γ (110) < γ (100). Careful examination of the individual grains also shows only slight misorientation between some of the grains in the *x*–*y* plane (azimuthal orientation) of the paper. On increasing the bias duration to 15 min, the fraction of grains that have identical *x*–*y* orientation is reduced quite drastically (not included in this paper but may be published in future), which confirmed that there is an optimum application of bias duration for nucleation and growth of the oriented and textured diamond crystals. In contrast, the diamond film grown using nucleation via ultrasonic agitation created a random distribution and orientation of the grains as shown in Fig. 1(b). These observations then prompted us to explore the nature of the diamond film texture in more detail using XRD pole figure measurements on samples of Fig. 1(a), (b).

The XRD setup shown in Fig. 8 can be used in different modes for experiments to determine texture of the film on a substrate. These include rocking curve and pole figure type of bell-shape measurements. In a rocking curve, the Bragg angle (2Θ) is fixed and the sample is slightly tilted or rocked and the XRD intensity is plotted as a function of the tilt angle. It produces a curve, which gives distribution of planes as a function of the tilt. The width of this curve gives information on the mosaic spread of the grains, which is used to assess epitaxial growth or preferred orientation. In rocking curve, only the planes close to parallel of the surface are measured. To assess the in-plane orientation, the pole figure is used in which both tilt and rotation are used to get a 3-dimensional nature of the texture. This is commonly referred to as Psi (Ψ) and Phi (Φ) scans. The sample is tilted in small Psi (Ψ) steps and rotated 360° in Phi (Φ) for each step. One can use a particular Bragg angle and obtain pole figure to obtain azimuthal alignment of a set of grans within the plane of a film. This is so-called Phi (Φ) scan and we have used it for measuring texture of diamond films of this study.

To study the crystal orientation of the film, XRD pole figure diagrams (Phi-Φ-Psi-Ψ) scans) and Phi (Φ) scans were performed on the diamond films of Fig. 1. The results of Phi (Φ) scans of diamond films of Fig. 1(a), (b) are presented in Fig. 1(c). It shows Phi scans from the BEN and the ultrasonically nucleated diamond films over a range of 360 degrees along with the scan from the silicon substrate. The FWHM (full width at half-maxima) of the diamond peak for the BEN sample is about 10° and is significantly larger than that of the silicon substrate. The XRD Phi scan used silicon (111) and diamond (111) planes from the 10 μm thick diamond BEN film and the results in Fig. 1(c)

TABLE 1: Processing conditions used for the carburization, BEN, and growth of diamond films.

Deposition parameters	Hydrogen etching	Carburization	Bias-enhanced nucleation	Growth
Duration of step (mins)	15	60	5 or 10	480
Bias voltage (V)	0	0	150–250	0
Substrate temperature (°C)	750	750	750	750
Pressure (Pa)	2666.4	2666.4	2666.4	12,670
H_2 flow (sccm)	100	100	100	39
CH_4 flow (sccm)	0	2	4	1
Ar flow (sccm)	0	0	0	60
Microwave power (Watts)	500	600	600	900

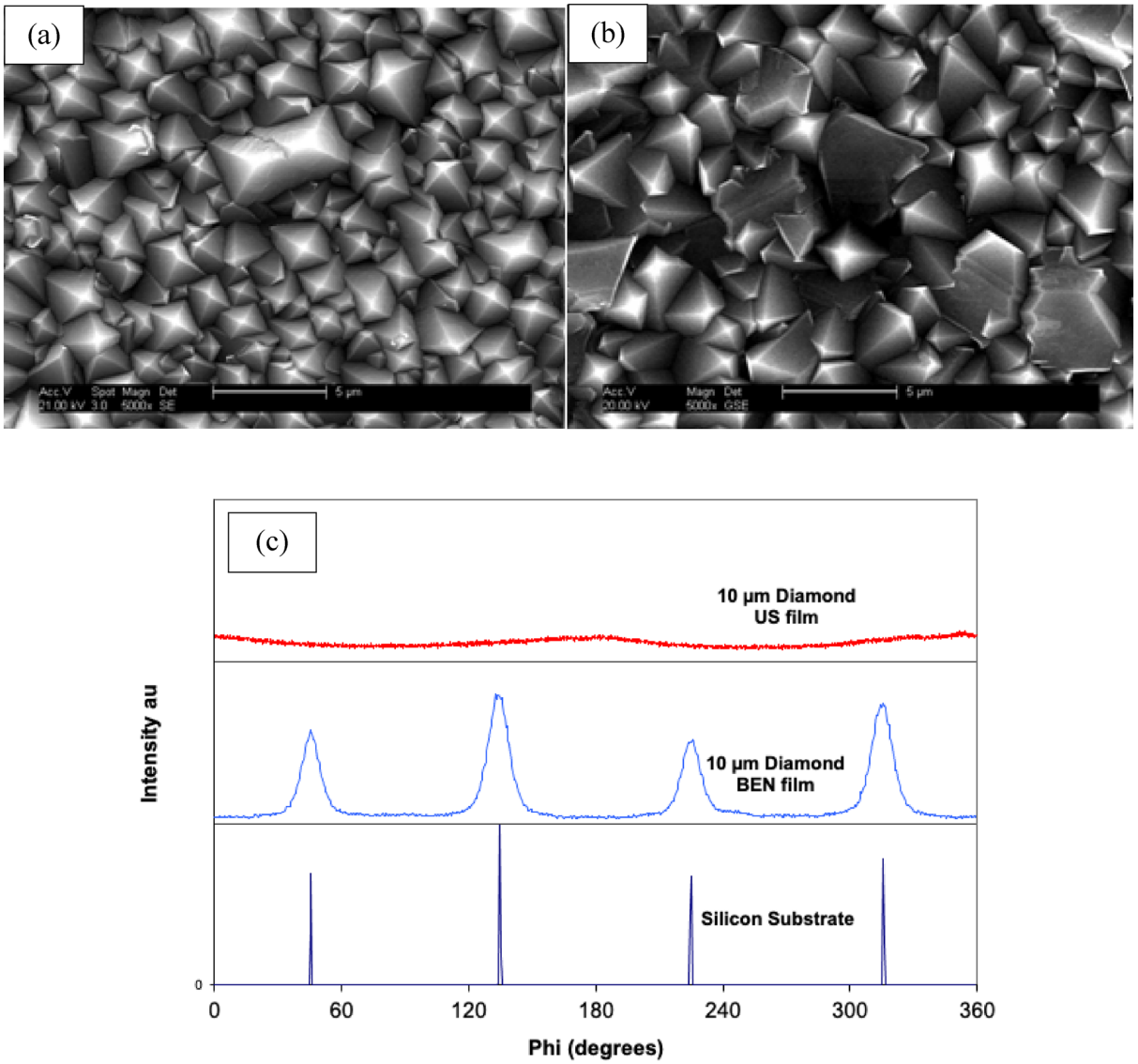

Figure 1: SEM of (a) an oriented diamond film nucleated by BEN at 150 V for 5 min and subsequently grown using MPECVD on Si (100) substrate. A majority of the diamond crystal are oriented similarly in the x–y plane (azimuthal orientation) leading to high degree of pyramidal-shape texture, (b) the randomly oriented diamond film nucleated using ultrasonic agitation and grown under conditions identical to (a), and (c) the XRD Phi scan of silicon (111) and diamond (111) planes from the 10 µm thick diamond BEN film indicating the preferential orientation of diamond planes (D)(100)// Si(100) and directions D < 100 > //Si < 100 > . The Phi scan from a randomly oriented 10 µm thick diamond film grown after nucleation by ultrasonic activation in a diamond slurry is also included for comparison showing a random orientation.

show 4 peaks 90° apart from Si substrate and BEN diamond film indicating the preferential alignment of diamond planes (D)(100)//Si(100) and directions D < 100 > //Si < 100 > . The Phi scan from a randomly oriented 10 µm diamond film grown after nucleation by ultrasonic activation in a diamond slurry is also included for comparison showing a random texture and orientation of the diamond film.

The quality of diamond film nucleated by BEN on Si(100) substrate improved with thickness as evident from the lower FWHM of the X-ray diffraction peak. The data in Fig. 2(a) are for a 2 µm thick film and in Fig. 2(b) are for a 10 µm thick film. We investigated this aspect by growing diamond films of two different thicknesses and examining by XRD pole figure measurements. The results of the pole figure diagram for the 2 µm and 10 µm thick diamond films nucleated by BEN and grown on the silicon substrate along with the diagram from Si (100) are shown in Fig. 2(a)–(c), respectively. Note the improvement in the sharpness of the peaks with the increase in thickness of the diamond film. Also, note that the peaks of the 10 µm thick BEN diamond film and Si substrate coincide with the same Phi-Psi values, confirming the close orientation relationship between the substrate and diamond film grown on it. These results also

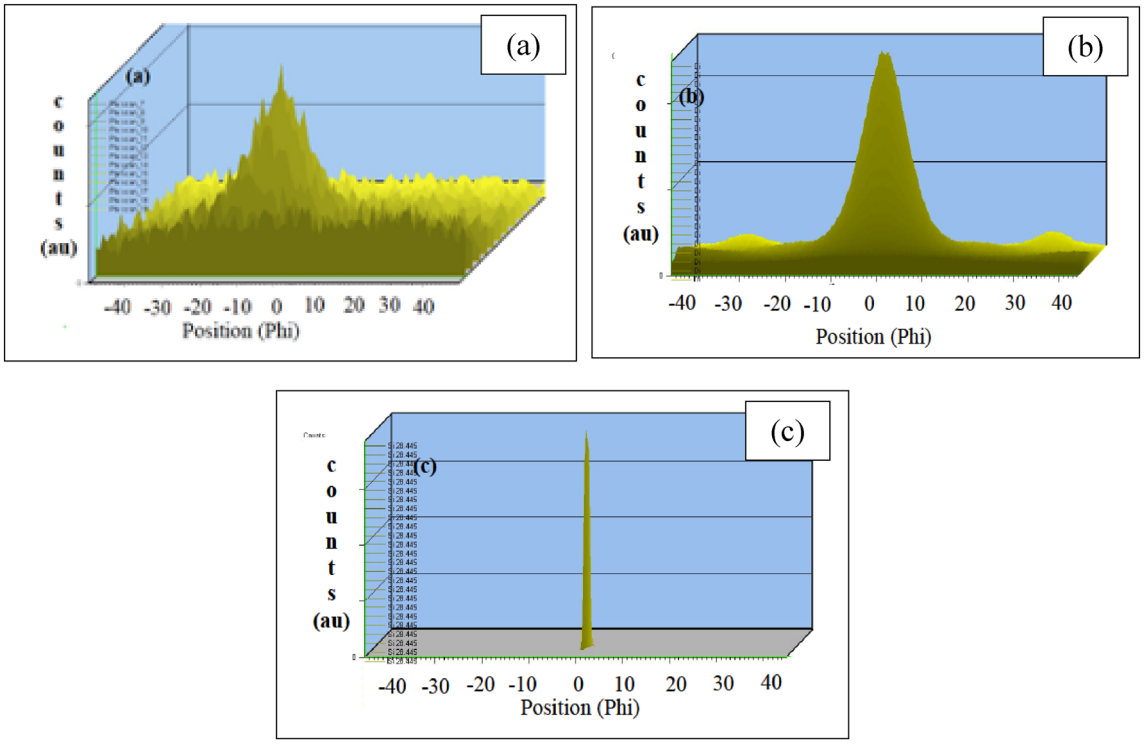

Figure 2: (111) XRD pole figure diagram (Phi-Psi scan) of (a) a 2-µm oriented film grown using BEN, (b) the 10-µm oriented film grown using BEN, and (c) the silicon substrate of the 10-µm BEN film. Note increase in the sharpness of the peak with diamond film growth.

suggest that the quality of the diamond film can be further improved by growing thicker films as reported by others [8. 9. 41].

Influence of applied voltage during BEN on the texture of diamond films

The SEM images in Fig. 3(a)–(c) show the effect of increasing applied voltage during BEN stage on the morphology of the diamond films. The BEN and all other processing parameters were held the same (time of BEN 10 min, 4sccm CH_4, 750 °C) for films shown except the applied voltage used during BEN. The BEN voltages of 150, 200 and 250 were applied during BEN for films shown in Fig. 3(a)–(c), respectively. The SEM images (Fig. 3) show that the azimuthal orientation of the film in x–y plane improved significantly at lower bias voltages. This is also confirmed by a visual count of the percentage of oriented grains shown in Fig. 4. This was determined by the examination of the SEM micrographs and counting the grains showing azimuthal alignment as well as the total number of grains. The ratio of these measurements provided the % alignment presented in Fig. 4. It shows that about 70%, 25%, and 7% of the grains have similar azimuthal orientation/texture that were created by the 150, 200, and 250 V applied during BEN, respectively. Therefore, an optimum level of the voltage during BEN is helpful for maximizing azimuthal texture of the diamond grains and films processed by MPECVD.

The texture of the diamond films grown after BEN at different voltages was measured using XRD Phi scans. Figure 5 shows the results of the XRD Phi scans of the films as a function of the bias voltages of 150, 200, and 250 V. Clearly, the azimuthal texture of the films is found to deteriorate with increasing bias voltage. The film nucleated at 150 V shows four diamond (111) peaks at 90° intervals, coinciding with the silicon (111) peak positions, indicating high degree of the azimuthal texture. As the bias voltage is increased, the orientation is found to be significantly poorer. The possible reason for a better azimuthal texture at lower biasing voltage is discussed next.

The role of bias during epitaxial growth of diamond has been extensively debated. The bias has been suggested to be responsible for epitaxy due to ion bombardment causing improved surface diffusion of adatoms or movement and rotation of nuclei. Chopra [39] has suggested that bias causes surface charge buildup on the forming nuclei thereby increasing its effective surface energy and consequently lowering the wetting angle of the nuclei formed and improving the chances of epitaxy, which could be debated lacking experimental verification. Other mechanisms suggested ion bombardment-assisted preferential etching of misoriented nuclei due to poorer bonding with the substrate or increased H^+ concentration in the plasma.

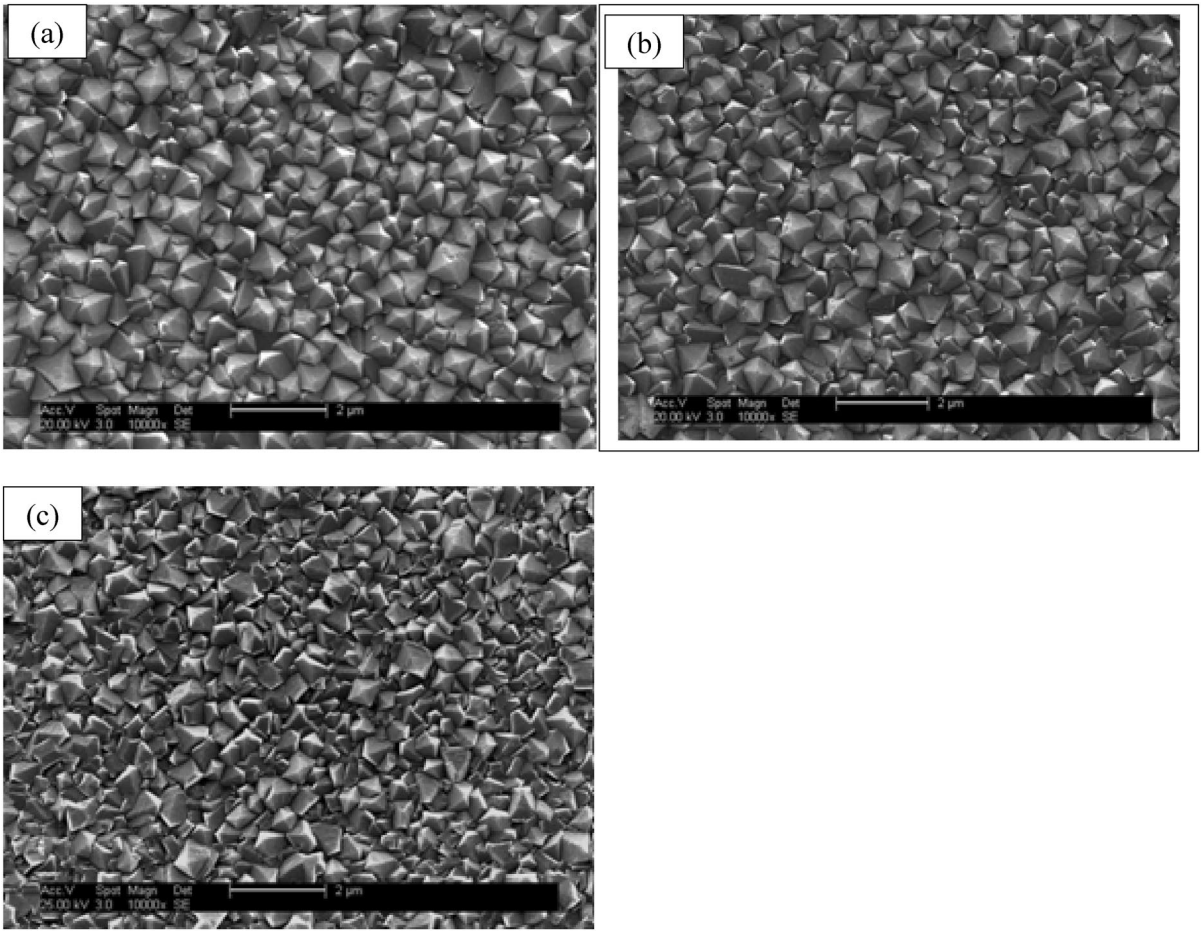

Figure 3: SEM micrographs showing the effect of BEN voltage (a) 150 V, (b) 200 V, and (c) 250 V on the azimuthal orientation and morphology of the grown diamond films. Other BEN parameters are constant (BEN 10 min, 4sccm CH_4, 750 °C).

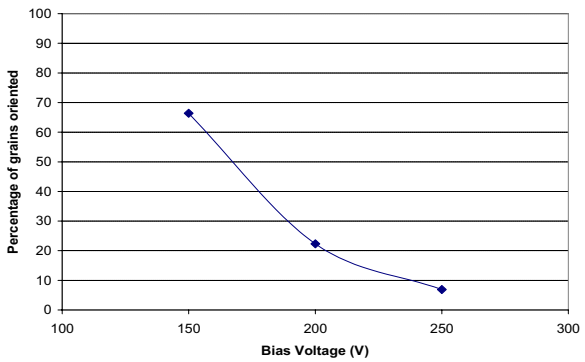

Figure 4: Variation in the percentage of oriented grains within x–y plane (azimuthal texture) as a function of the bias voltage applied during the BEN step measured from SEM photographs. Orientation is found to improve with lower bias voltage. Other BEN parameters are constant (BEN 10 min, 4sccm CH_4, 750 °C).

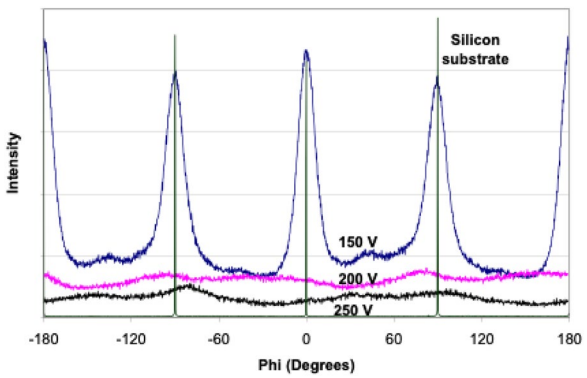

Figure 5: XRD Phi scans showing the effect of BEN voltage on the orientation and texture of diamond films deposited. Clearly, the orientation deteriorates with increasing voltage. Other BEN parameters are constant (BEN 10 min, 4sccm CH_4, 750 °C).

Higher applied voltage during BEN generally leads to higher diamond nucleation density on Si wafers based on our research work as well as of other researchers [42, 44–46, 48].

While the exact mechanism of BEN is not understood, the application of an electrical bias field/voltage accelerates the positively charged radicals toward the substrate and provides sufficient energy for overcoming the nucleation barrier

thereby promoting diamond nucleation. In addition, diamond nucleation under BEN conditions occurs within the carbon film formed during the carburization and BEN steps (Table 1) based on our recent research [47]. Our research has shown that the diamond nuclei form epitaxially in the carbon film in the vicinity of the Si substrate. At this stage, these nuclei are also free to rotate azimuthally within the x–y plane thereby creating oriented nuclei. Then, these nuclei grow vertically in the z direction and coalesce to form a continuous diamond film showing azimuthal texture [47]. Since the density of diamond nucleus is small at lower applied potential during BEN, these nuclei grow during the remaining MPECVD processing period without changing their azimuthal orientation. In contrast, the higher voltages during BEN create many more diamond nuclei of possibly different azimuthal orientations. These nuclei upon further growth then lead to poorer azimuthal texture. It is also possible that the adhesion force between the Si substrate and diamond nuclei will be higher at higher applied potential during BEN and too high an electric field is expected to restrict free rotation of the diamond nuclei thereby leading to poor azimuthal texture. Based on this argument, it is suggested that an optimum applied voltage or electric field during BEN is expected to promote nucleation of diamond on Si that can rotate freely to lead to high degree of azimuthal texture as observed in this study. Another factor that should also be considered is that plasma etching is taking place simultaneously and dynamically with continued diamond deposition (after BEN step) for further growth of diamond in a MPECVD environment leading to textured films. The plasma etching is expected to etch away sp^2-bonded carbon and misoriented diamond nuclei as well more effectively in samples with lower diamond nuclei density (lower voltage in BEN) than having the higher density of nuclei created at higher voltages. The process of nucleation in a BEN approach is a dynamic process in which the time of application of the bias voltage, the magnitude of the bias voltage, carbon precursor (CH_4) concentration, and plasma etching play important roles in the diamond nucleation, growth, and evolution of textured film. Each of these parameters has to be optimum in order to synthesize diamond films having epitaxial and azimuthal textures as described and shown in Figs. 1, 2, 3, 4, and 5. These aspects are also relevant and applicable to wide area processing of diamond single crystal wafers using Ir nucleation layer on Si and other substrates [44–46].

Figure 6 shows the Raman spectra from the BEN films biased for various times along with the diamond film nucleated by ultrasonic (US) activation. All the spectra show the 1st-order diamond phonon peak at 1332 cm^{-1} wave number. But the BEN films show another broader peak because of the sp^2 carbon around 1550 cm^{-1}. It is known that the Raman scattering cross-section is significantly higher (by a factor of 100) for the sp^2 carbon bonding as compared to the sp^3 carbon bonds. This

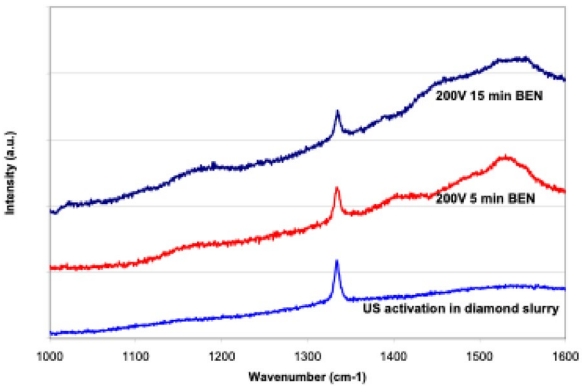

Figure 6: Raman spectra of diamond films grown after nucleation using BEN at 200 V for 5 min and 200 V for 15 min. Also, diamond film grown under identical conditions but nucleated using ultrasonic (US) nucleation is shown.

difference is used during quantitative analysis of diamond films in which the intensity or area from sp^2 carbon peak is divided by 100 to calculate the content of the sp^2 carbon [28, 29]. While we see sp^2 peak in the Raman spectra at 1550 cm^{-1}, the actual sp^2 content in the film is not significant because of this aspect. This difference between the spectra of the BEN diamond and ultrasonically nucleated films could be due to the higher flow rates of methane used during the carburization and biasing steps, which are not required for the ultrasonically nucleated films. The Raman spectra of the various BEN films are largely identical with a first-order diamond peak at 1332 cm-1 and a broad peak around 1550 cm^{-1}.

Perspective on textured diamond film for quantum applications and wafer scale single crystal diamond

The findings from this research are important for processing diamond containing nitrogen vacancy centers (NV) for quantum devices. As described earlier, the NV centers in diamond are generally oriented randomly along four possible < 111 > directions. There is a need to preferentially orient NV centers along one of the four < 111 > directions. The oriented NV centers are desirable for enhancing detectability for quantum application using ODMR and the azimuthally textured diamond film should help toward this goal. The results obtained from this research have demonstrated a fundamental understanding of processing conditions for texturing of the diamond films in situ using bias-enhanced nucleation (BEN) followed by growth using MPECVD. It is hypothesized that such a textured diamond film should encourage creation of aligned NV centers during processing and in situ doping by nitrogen in a MPECVD approach. This approach also required a fundamental understanding of the role of the diamond nucleation and growth mechanisms on Si substrates as described in our recent paper [47] to achieve the goal of azimuthally textured diamond film.

Researchers have used HPHT-synthesized tiny diamond crystals and then diamond film is grown on these diamond crystals. Then nitrogen is implanted and annealed at high temperatures (1200–1500 °C) to create NV centers. This approach complicates processing for devices and limits widespread applications to quantum devices and systems. In this context, polycrystalline diamond film is of great interest for creating NV defect, but their quality has to be significantly improved. Our research on azimuthally textured polycrystalline diamond film is expected to provide this opportunity for creating oriented NV centers for many applications. Our approach has shown that azimuthally textured polycrystalline diamond film of good quality can be processed through understanding of the nucleation mechanism of BEN followed by growth. This is consistent with the vast amount of data in the literature on related processing and properties of textured diamond film as evident from several recent papers [42, 44–46]. Based on the results of this research, we plan to explore in situ doping of nitrogen during growth by MPECVD for creating negatively charged NV centers. The texture of diamond crystals grown in *Z*-direction and XY plane can be controlled using some of our approaches presented here, which are expected to offer many more possibilities for achieving preferred orientation of the NV centers in diamond for applications in quantum systems. The optimum nitrogen doping level has to be determined but it should not be too high for preserving the diamond crystal structure. The quality of NV centers thus created will be characterized by ODMR and PL (photoluminescence) techniques, which will provide feedback on the processing of the optimum quality NV centers in diamond films by MPECVD.

As mentioned earlier, there is great deal of interest and excitement worldwide on the prospects for processing of large diameter (50 and 100 mm) single crystal diamond for a myriad of current and futuristic devices useful for commercial and defense applications. Recent successes in processing 92 mm single crystal diamond rely on the BEN approach for nucleating epitaxial diamond on substrates such as Si (100)/YSZ/Ir/diamond or on Si (100)/$SrTiO_3$/Ir/diamond [44–46]. The role of Ir in these approaches has been that BEN approach leads to epitaxial nuclei of similar azimuthal texture within the carbon film on Ir. There is smaller (~ 7%) lattice mismatch between diamond and Ir, which promotes lateral growth by domain-matching epitaxy [6] leading to wider-area epitaxy of diamond upon further growth in a MPECVD. Further understanding of the BEN mechanism on Si and other substrates is expected to advance processing of wafer scale diamond single crystal as well. Therefore, our research described in this paper should be helpful in applications of diamond for quantum systems, and as a substrate for ultra-wide bandgap semiconductor electronics.

Conclusions

The roles of bias-enhanced nucleation (BEN) and nucleation by ultrasonic agitation followed by growth were studied in this paper for processing of oriented diamond film with azimuthal texture by MPECVD on Si (100) wafers. Highly textured diamond films were obtained on Si (100) using BEN. In contrast, the ultrasonic nucleation led to a random orientation and no texture. In addition, the role of applied voltage during BEN on the texture of diamond films was also studied using the SEM and XRD pole figure measurements. The results showed that lower applied potential of 150 V led to films with high degree of the azimuthal orientation of the diamond grains than the higher applied potentials (200 and 250 V). Almost 70% of the diamond grains had azimuthal orientation at 150 V compared to only 25% and 7% orientation, respectively, at 200 V and 250 V. The surface morphology of the diamond crystals/grains was studied using SEM, which indicated pyramidal diamond grain shape having the base parallel to (100) plane and pyramidal faces along (111) planes that are consistent with the highly oriented texture data from X-ray pole figure. Raman spectroscopy results from diamond films showed strong Raman peaks at ~ 1332 cm^{-1}, which attested to good quality of the diamond films. The results showed that diamond films of optimum quality can be processed upon in situ doping containing nitrogen vacancy (NV) centers. Furthermore, these results provided a fundamental understanding on the nucleation and growth of textured diamond films of improved quality for a myriad of applications in quantum systems and relevance to wafer scale processing of diamond single crystal.

Experimental methods

The diamond films were processed in an MPECVD system model ASTEX AX5100, which has been described in several of our publications [22–30]. Two types of diamond nucleation approaches were studied. The first used an ultrasonic agitation approach in which 20 g (20–40 μm) diamond powder in 100 ml ethanol slurry was placed in beaker and ultrasonicated for 2 h followed by a thorough rinse in DI water, acetone, and ethanol followed by growth. The second approach used BEN for which the MPECVD system was modified for applying the electrical bias or voltage required for BEN as schematically shown in Fig. 7. It used 2 mm diameter circular molybdenum wire ring on which a wire mesh screen made of 0.3 mm diameter molybdenum wire was held. This wire mesh was inserted into the MPECVD chamber and held 20 mm above the substrate. The screen mesh was connected to one terminal of an MDX-500 DC power supply though an electrical

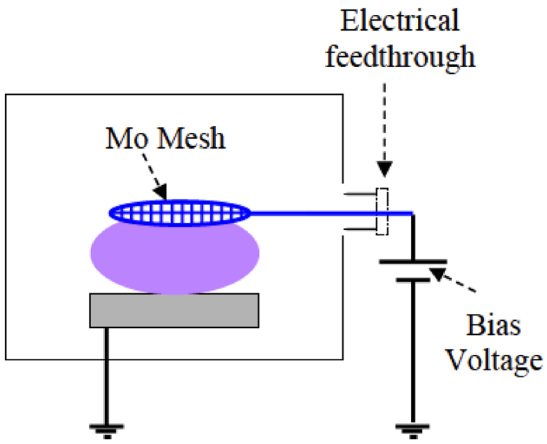

Figure 7: Schematic of the setup used for bias-enhanced nucleation (BEN) of diamond in the MPECVD system.

feed-through. The substrate holder and the MPECVD chamber were grounded as was the other terminal of the power supply.

All experiments were performed on p-type silicon (100) wafers diced into 2.54 cm by 2.54 cm squares as substrates. The substrates were etched in a standard hydrofluoric–nitric–acetic (HNA) acid solution (20 ml HF + 60 ml HNO_3 + 160 ml CH_3COOH) to remove any contaminated top layer. This was followed by cleaning the silicon pieces in 2% HF solution in DI water to remove the native oxide layer before silicon pieces were placed inside the deposition chamber. The MPECVD system chamber was evacuated to a base pressure of at least 1×10^{-5} Pa at the processing temperature of 750 °C. The silicon was then etched in hydrogen plasma for 15 min at 2666.44 Pa, 100 sccm H_2 flow, and 500 Watts microwave power to remove surface impurities. This was followed by a carburization step for 60 min in which 2 sccm of CH_4 was introduced into the chamber and the microwave power was increased to 600 Watts. Then, the bias voltage between 150 and 250 V was applied to the molybdenum screen mesh though the electrical feed-through. The duration of the bias step was varied in the experiments. After the nucleation enhancement steps, the samples were placed in the deposition chamber and this time the mesh was removed. Diamond films were grown on the pre-nucleated wafers in a 900W plasma of H_2-Ar-CH_4 mixture at the ratio of 39-60-1 and at a pressure of 12,670 Pa. The substrate temperature as measured by a thermocouple below the substrate holder was set at 750 °C. The growth step was carried out for 8 h followed by 15 min of hydrogen plasma etching to remove the carbon deposits. The growth conditions were selected based on the previous results that showed well-crystallized diamond grains with low secondary nucleation [47]. A summary of the process conditions is given in Table 1.

The XRD was used for identification of the diamond phase formation on the substrates, as well as for studying the

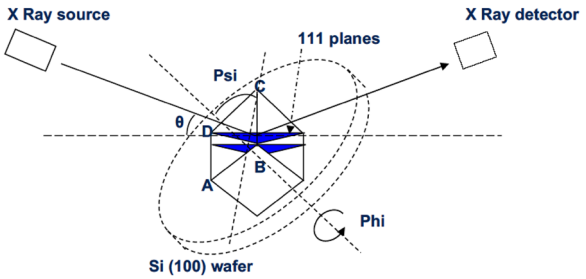

Figure 8: Schematic of the XRD setup for measuring texture using pole figures and Psi (Ψ) and Phi (Φ) scans.

orientation/texture using XRD pole figure measurements and XRD Phi scans. A Panalytical Xpert-Pro system with a hybrid monochromator and a 1.54A° Copper Kα X-ray source was used for the study. A schematic of the XRD setup, sample and the various axes of rotation is shown in Fig. 8. More details on the Phi scans for determining texture and azimuthal crystal orientation are provided in the results and discussion section and reference [49].

Raman spectroscopy measurements were made using a model T 64000 Jobin Yvon triple monochromator system equipped with an Olympus BX-41 microscope attachment. The Raman scattering was performed using 514.5 nm Ar^+ ion laser. The samples were characterized by a Philips XL-30 FEG Environmental Scanning Electron Microscope (ESEM).

Acknowledgments

This material is based on work supported by the National Science Foundation under NSF Award Numbers: 2103058 and 2126275. Any opinions, findings, and conclusions or recommendations expressed in this material are those of the authors and do not reflect views of the National Science Foundation.

Author contributions

VSJ: Data curation (equal); Formal analysis (equal); Investigation (equal); Methodology (equal); Validation (equal); Writing - first draft (equal). RNS: Conceptualization; Formal analysis (equal); Funding acquisition; Investigation (equal); Methodology (equal); Project administration; Resources; Supervision; Validation (equal); Writing - final draft. Funding: This material is based on work supported by the National Science Foundation under NSF Award Numbers: 2103058 and 2126275. Any opinions, findings and conclusions or recommendations expressed in this material are those of the authors and do not reflect views of the National Science Foundation.

Data availability

The data will be made available at reasonable request.

Declarations

Conflict of interest The authors declare that they have no known competing financial interests or personal relationships that could have appeared to influence the work reported in this paper.

References

1. D. Das, R.N. Singh, A review on nucleation, growth, and low-temperature synthesis of diamond thin films. Int. Mater. Rev. **52**(2), 1–37 (2007)
2. S. Samantaray, R.N. Singh, A review of synthesis and properties of cubic boron nitride thin films. Int. Mater. Rev. **50**(6), 313–344 (2005)
3. M. Jana, R.N. Singh, A review: Progress in CVD synthesis of layered hexagonal boron nitride with tunable properties and their applications. Int. Mater. Rev. (2017). https://doi.org/10.1080/09506608.2017.1322833
4. J. Narayan, A. Bhaumik, Novel phase of carbon, ferromagnetism, and conversion into diamond. J. Appl. Phys. **118**, 215303 (2015)
5. A. Bhaumik, R. Sachan, J. Narayan, Tunable charge states of nitrogen-vacancy centers in diamond for ultrafast quantum devices. Carbon **142**, 662–672 (2019)
6. J. Narayan, A. Bhaumik, S. Gupta, P. Joshi, P. Riley, R.J. Narayan, Role of Q-carbon in nucleation and formation of continuous diamond film. Carbon **176**, 558–568 (2021)
7. J. Wrachtrup, F. Jelezko, Processing quantum information in diamond. J. Phys. Condens. Matter. **18**(21), 807–824 (2006)
8. B. Hensen, H. Bernien, A.E. Dréau, A. Reiserer, N. Kalb, M.S. Blok, J. Ruitenberg, R.F.L. Vermeulen, R.N. Schouten, C. Abellán, W. Amaya, V. Pruneri, M.W. Mitchell, M. Markham, D.J. Twitchen, D. Elkouss, S. Wehner, T.H. Taminiau, R. Hanson, Experimental loophole-free violation of a Bell inequality using entangled electron spins separated by 1.3 km. Nature **526**(7575), 682–686 (2015)
9. M. Hirose, P. Cappellaro, Coherent feedback control of a single qubit in diamond. Nature **532**(7597), 77–80 (2016)
10. B.M. Chang, H.H. Lin, L.J. Su, W.-D. Lin, R.J. Lin, Y.K. Tzeng, R.T. Lee, Y.C. Lee, A.L. Yu, H.C. Chang, Highly fluorescent nanodiamonds protien-functionalized for cell labelling and targeting. Adv. Funct. Mater. **23**(46), 5737–5745 (2013)
11. J.R. Maze, P.L. Stanwix, J.S. Hodges, S. Hong, J.M. Taylor, P. Cappellaro, L. Jiang, M.V.G. Dutt, E. Togan, A.S. Zibrov, A. Yacoby, R.L. Walsworth, M.D. Lukin, Nanoscale magnetic sensing with an individual electronic spin in diamond. Nature **455**(7213), 644–647 (2008)
12. A. Gruber, A. Dräbenstedt, C. Tietz, L. Fleury, J. Wrachtrup, C. Borczyskowski, Scanning confocal optical microscopy and magnetic resonance on single defect centers. Science **276**(5321), 2012–2014 (1997)
13. E. Neu, D. Steinmetz, J. Riedrich-Möller, S. Gsell, M. Fischer, M. Schreck, C. Becher, Single photon emission from silicon-vacancy colour centres in chemical vapour deposition nanodiamonds on iridium. New J. Phys. **13**, 25012 (2011)
14. I. Lovchinsky, A.O. Sushkov, E. Urbach, N.P. de Leon, S. Choi, K. De Greve, R. Evans, R. Gertner, E. Bersin, C. Müller, L. McGuinness, F. Jelezko, R.L. Walsworth, H. Park, M.D. Lukin, Nuclear magnetic resonance detection and spectroscopy of single proteins using quantum logic. Science **351**(6275), 836–841 (2016)
15. C.G. Yale, B.B. Buckley, D.J. Christle, G. Burkard, F.J. Heremans, L.C. Bassett, D.D. Awschalom, All-optical control of a solid-state spin using coherent dark states. Proc. Natl. Acad. Sci. U.S.A. **110**(19), 7595–7600 (2013)
16. H. Bernien, B. Hensen, W. Pfaff, G. Koolstra, M.S. Blok, L. Robledo, T.H. Taminiau, M. Markham, D.J. Twitchen, L. Childress, R. Hanson, Heralded entanglement between solid state qubits separated by three meters. Nature **497**(7447), 86–90 (2013)
17. P.C. Maurer, G. Kucsko, C. Latta, L. Jiang, N.Y. Yao, S.D. Bennett, F. Pastawski, D. Hunger, N. Chisholm, M. Markham, D.J. Twitchen, J.I. Cirac, M.D. Lukin, Room-temperature quantum bit memory exceeding one second. Science **336**(6086), 1283–1286 (2012)
18. A. Haque, S. Sumaiya, An overview on the formation and processing of nitrogen-vacancy photonic centers in diamond by ion implantation. J. Manuf. Mater. Process. **1**(6), 1–16 (2017)
19. V.N. Mochalin, O. Shenderova, D. Ho, Y. Gogotsi, The properties and applications of nanodiamonds. Nat. Nanotechnol. **7**(1), 11–23 (2012)
20. J.-P. Boudou, P.A. Curmi, F. Jelezko, J. Wrachtrup, P. Aubert, M. Sennour, G. Balasubramanian, R. Reuter, A. Thorel, E. Gaffet, High yield fabrication of fluorescent nanodiamonds. Nanotechnology **20**(23), 235602 (2009)
21. Y. Chu, N. de Leon, B. Shields, B.J.M. Hausmann, R. Evans, M.J. Burek, M. Markham, A. Stacey, A. Zibrov, D. Twitchen, M. Loncar, H. Park, P. Maletinsky, M.D. Lukin, Coherent optical transitions in implanted nitrogen vacancy centers. Nano Lett. **14**, 1982–1986 (2014)
22. N. Govindaraju, R.N. Singh, Effect of microwave plasma process conditions on nanocrystalline diamond deposition on AlGaN/GaN HEMT and Si device metallizations. Ceram. Trans. **234**, 99–113 (2012)
23. N. Govindaraju, D. Das, R.N. Singh, P.B. Kosel, Comparison of the electrical behavior of AlN-on-diamond and AlN-on-Si MIS rectifying structures. Ceram. Trans. **235**, 77–86 (2012)
24. N. Govindaraju, P.B. Kosel, R.N. Singh, Effect of nanocrystalline diamond deposition conditions on Si MOSFET device characteristics. Ceram. Trans. **235**, 87–93 (2012)
25. N. Govindaraju, R.N. Singh, Processing of nanocrystalline diamond thin films for thermal management of wide bandgap

semiconductor power electronics. Mater. Sci. Eng. B **176**(14), 1058–1072 (2011)
26. N. Govindaraju, C. Kane, R.N. Singh, Processing of multilayered nanocrystalline and microcrystalline diamond thin films using Ar-rich microwave plasmas. J. Mater. Res. **26**(24), 3072–3082 (2011)
27. N. Govindaraju, D. Das, P.B. Kosel, R.N. Singh, High-temperature dielectric behavior of nanocrystalline and microcrystalline diamond thin films. ECS Trans. **33**(13), 155–168 (2010)
28. N. Govindaraju, D. Das, R.N. Singh, P.B. Kosel, High-temperature electrical behavior of nanocrystalline and microcrystalline diamond films. J. Mater. Res. **23**(10), 2774–2786 (2008)
29. D. Das, R.N. Singh, S. Chattopadhyay, K.H. Chen, Thermal conductivity of diamond films deposited at low surface temperatures. J. Mater. Res. **21**(9), 2379–2388 (2006)
30. D. Das, V. Jayaseelan, R. Ramamurti, R.S. Kukreja, L. Guo, R.N. Singh, Low surface temperature synthesis and characterization of diamond thin films. Diam. Relat. Mater. **15**, 1336–1349 (2006)
31. B.R. Stoner, G.-H.M. Ma, S.D. Wolter, J.T. Glass, Characterization of bias-enhanced nucleation of diamond on silicon by in vacuo surface analysis and transmission electron microscopy. Phy. Rev B **45**(19), 11047–11084 (1992)
32. A. Saravanan, B.R. Huang, K.J. Sankaran, S. Kunuku, C.L. Dong, K.C. Leou, N.H. Tai, I.N. Lin, Bias-enhanced nucleation and growth processes for ultrananocrystalline diamond films in Ar/CH_4 plasma and their enhanced plasma illumination properties. ACS Appl. Mater. Interfaces **6**(13), 10566–10575 (2014)
33. K. Janischowsky, W. Ebert, E. Kohn, Bias enhanced nucleation of diamond on silicon (100) in a HFCVD system. Diam. Relat. Mater. **12**, 336–339 (2003)
34. W. Kulisch, L. Ackerman, B. Sobisch, On the mechanisms of bias enhanced nucleation of diamond. Phys. Status Solidi (a) **154**, 155–174 (1996)
35. S. Yugo, T. Kanai, T. Kimura, T. Muto, Generation of diamond nuclei by electric field in plasma chemical vapor deposition. Appl. Phys. Lett. **58**(10), 1036–1038 (1991)
36. N. Ishigaki, S. Yugo, Mechanism of diamond epitaxial growth on Silicon. Diam. Relat. Mater. **9**, 1646–1649 (2000)
37. X. Jiang, K. Schiffmann, A. Westphal, C.P. Klages, Atomic force microscopic study of heteroepitaxial diamond nucleation on (100) silicon. Appl. Phy. Lett. **63**(9), 1203–1205 (1993)
38. Y.K. Kim, K.H. Lee, M.J. Lee, J.Y. Lee, The nucleation of highly oriented diamond on silicon using a negative bias. Thin Solid Films **341**, 211–215 (1999)
39. B. Golding, C. Bednarski-Meinke, Z. Dai, Diamond heteroepitaxy: Pattern formation and mechanisms. Diam. Relat. Mater. **13**, 545–551 (2004)
40. K.L. Chopra, *Thin Film Phenomena*, 3rd edn. (McGrow Hill, New York, 1969)
41. G. Chikvaidze, N. Mironova-Ulmane, A. Plaude, O. Sergeev, Investigation of silicon carbide polytypes by Raman spectroscopy. Latvian J. Phys. Tech. Sci. (2014). https://doi.org/10.2478/lpts-2014-0019
42. S. Mandal, Nucleation of diamond films on heterogeneous substrates: a review. RSC Adv. **11**, 10159 (2021). https://doi.org/10.1039/d1ra00397f
43. S.A. Linnik, A.V. Gaydaychuk, A.S. Mitulinsky, S.P. Zenkin, Radio frequency bias enhanced nucleation of CVD diamond. Mater. Lett. **324**, 132670 (2022)
44. M. Schreck, S. Gsell, R. Brescia, M. Fischer, Ion bombardment induced buried lateral growth: the key mechanism for the synthesis of single crystal diamond wafers. Sci. Rep. **7**(1), 44462 (2017)
45. J.-C. Arnault, S. Saada, V. Ralchenko, Chemical vapor deposition single-crystal diamond: a review. Phys. Status Solidi RRL **16**, 2100354 (2022). https://doi.org/10.1002/pssr.202100354
46. W. Jaeger, Advanced and in situ transmission electron microscopy of diamond: A review. In: Semiconductors and Semimetals, Volume 104, 31 (2021), ISSN 0080–8784 https://doi.org/10.1016/bs.semsem.2020.08.003
47. V.S. Jayaseelan, R.N. Singh, Diamond nucleation in carbon films on Si wafer during microwave plasma enhanced chemical vapor deposition for quantum applications. J. Appl. Phys. **133**(15), 155302 (2023)
48. Jean-Charles Arnault, and Hugues Girard, "Diamond Nucleation and Seeding Techniques: Two Complementary Strategies for the Growth of Ultra-thin Diamond Films", Oliver Williams. Nanodiamond, chapter 10 (31), RSC Nanoscience & Nanotechnology, pp.221–252, 2014, Nanoscience & Nanotechnology Series., 978–1–84973–639–8. https://doi.org/10.1039/9781849737616-00221. cea-01831889
49. G.F. Harrington, J. Santiso, Back-to-basics tutorial: X-ray diffraction of thin films. J. Electroceram. **47**(4), 141–63 (2021)